Elsevier Editorial System(tm) for Microbes and Infection
Manuscript Draft

Manuscript Number: MICINF-D-09-00249R1

Title: Japanese encephalitis virus down-regulates thioredoxin and induces ROS-mediated ASK1-ERK/p38 MAPK activation in human promonocyte cells

Article Type: Original article

Keywords: Japanese encephalitis virus, apoptosis, 2D/MS, thioredoxin, ASK1, ERK/p38 MAPK

Corresponding Author: Dr. Cheng-Wen Lin, PhD

Corresponding Author's Institution: China Medical University

First Author: Cheng-Wen Lin, PhD

Order of Authors: Cheng-Wen Lin, PhD

Abstract: Japanese encephalitis virus (JEV), a mosquito-borne flavivirus, causes severe neurological disease with high mortality. Molecular mechanisms of JEV pathogenesis such as upstream apoptotic processes and pathways are not yet completely resolved or understood. In this study, JEV replication in human promonocyte cells induced time-dependent apoptosis and activated virus dose-dependent caspases 3, 8 and 9. Proteomic analysis demonstrated up- and down-regulated (more or less than 1.5-fold) proteins in JEV infected promonocyte cells. Biological process categorization showed processes of antioxidation, free radical removal, and sulfur redox metabolism entailed many identified up- and down-regulated proteins. Down-regulation of thioredoxin, confirmed by using Western blotting, was involved in the apoptosis process of the oxidative stress response pathway. JEV infection caused increased intracellular ROS production and activation of ASK1-ERK/p38-MAPK signaling. ERK/p38 MAPK inhibitor PD98059 treatment definitely suppressed this apoptosis. Down-regulation of thioredoxin, intracellular ROS increase, and activation of ASK1-ERK/p38 MAPK signaling were associated with JEV-induced apoptosis, all helpful for elucidating the cellular and molecular basis of JE pathogenesis.

2010/02/08

Japanese encephalitis virus down-regulates thioredoxin and induces ROS-mediated ASK1-ERK/p38 MAPK activation in human promonocyte cells

Tsuey-Ching Yang[1] Chien-Chen Lai [2, 3 +] Su-Lian Shiu[1] Pei-Hsin Chuang[1]
Bo-Cheng Tzou[1] Ying-Ya Lin[1] Fuu-Jen Tsai [2,¶] Cheng-Wen Lin [1,4,5]

[1] Department of Medical Laboratory Science and Biotechnology, China Medical University, Taichung 404, Taiwan
[2] Department of Medical Genetics and Medical Research, China Medical University Hospital, Taichung, 404 Taiwan
[3] Institute of Molecular Biology, National Chung Hsing University, Taichung, 402 Taiwan
[4] Clinical Virology Laboratory, Department of Laboratory Medicine, China Medical University Hospital, Taichung, 404 Taiwan
[5] Department of Biotechnology, College of Health Science, Asia University, Wufeng, Taichung, Taiwan

*****Corresponding author: Cheng-Wen Lin, PhD, Professor. Department of Medical Laboratory Science and Biotechnology, China Medical University, No. 91, Hsueh-Shih Road, Taichung 404, Taiwan

Fax: 886-4-22057414.

Email: cwlin@mail.cmu.edu.tw

[+] **Co-first author.**

[¶]Additional corresponding author.

Abstract

Japanese encephalitis virus (JEV), a mosquito-borne flavivirus, causes severe neurological disease with high mortality. Molecular mechanisms of JEV pathogenesis such as upstream apoptotic processes and pathways are not yet completely resolved or understood. In this study, JEV replication in human promonocyte cells induced time-dependent apoptosis and activated virus dose-dependent caspases 3, 8 and 9. Proteomic analysis demonstrated up- and down-regulated (more or less than 1.5-fold) proteins in JEV infected promonocyte cells. Biological process categorization showed processes of antioxidation, free radical removal, and sulfur redox metabolism entailed many identified up- and down-regulated proteins. Down-regulation of thioredoxin, confirmed by using Western blotting, was involved in the apoptosis process of the oxidative stress response pathway. JEV infection caused increased intracellular ROS production and activation of ASK1-ERK/p38-MAPK signaling. ERK/p38 MAPK inhibitor PD98059 treatment definitely suppressed this apoptosis. Down-regulation of thioredoxin, intracellular ROS increase, and activation of ASK1-ERK/p38 MAPK signaling were associated with JEV-induced apoptosis, all helpful for elucidating the cellular and molecular basis of JE pathogenesis.

Keywords: Japanese encephalitis virus (JEV), apoptosis, 2D/MS, thioredoxin, ASK1, ERK/p38 MAPK

1. Introduction

Japanese encephalitis virus (JEV) is a member of the *Flaviviridae* family, including other key pathogens like dengue virus (DEN), yellow fever (YF), St. Louis encephalitis virus, Murray valley encephalitis virus (MVE), Langat virus, West Nile virus (WNV), and tick-borne encephalitis (TBE) virus [1, 2]. The JEV genome is a single-stranded, positive-sense RNA with about 11,000 nucleotides in length [2]. The single, long ORF of JEV genome encodes structural proteins (capsid (C), membrane (prM/M), and envelope (E)) plus non-structural (NS1, NS2A, NS2B, NS3, NS4A, NS4B, NS5). JEV is a mosquito-borne neurotropic flavivirus [1], causing severe central nervous system diseases: poliomyelitis-like acute flaccid paralysis, aseptic meningitis and encephalitis [3]. Japanese encephalitis (JE) shows 30% mortality, with about half the survivors have severe neurological sequelae [3]. Approximately 50,000 cases with 10,000 deaths are reported annually in Asia [1, 4]. Neuronal apoptosis and inflammation response are chiefly attributed to JEV-induced cytopathology [5] that causes pathogenesis of JE in humans, while mechanisms for activation of apoptosis and inflammation are not fully understood. Such infection triggers cell apoptosis: e.g., in astrocytes and neuronal cells [6-9]. Mechanisms of JEV-induced apoptosis have been reported, including initiation of endoplasmic reticulum stress [10], generation of reactive oxygen species (ROS), activation of nuclear factor kappa B (NF-kappaB) [7],

activation of caspase-8 in a FADD-independent manner, activation of caspase-9 by mitochondrion-dependent pathway [9], plus the engagement of tumor necrosis factor receptor-1 (TNFR-1) and TNFR associated death domain (TRADD) [8]. Molecular pathways and processes of apoptosis are critical to understanding JE pathogenensis.

Combined two-dimensional gel electrophoresis and mass spectrometry (2D-GE/MS) are available and successful approaches to identify changes in expression of proteins in virus-infected cells for locating pathophysiologic processes and pathways [11, 12]. Comparative proteome analysis based on 2D-GE/MS methods may better elucidate molecular mechanisms underlying pathological processes and pathways in JEV infection. We determined apoptosis-related protein profile in JEV-infected human promonocyte HL-CZ cells with 2D-GE/MS, then characterized pathological processes and pathways induced by JEV and further analyzed via PANTHER (Protein ANalysis THrough Evolutionary Relationships) Classification. Down-regulated thioredoxin confirmed using Western blotting could associate with intracellular ROS production and ASK1/p38-MAPK activation of signaling in the JEV-infected apoptosis.

2. Materials and methods

2.1. Viruses and cells

JEV strain T1P1 was used as previously described [13]. Vero cells for JEV

amplification were maintained in Dulbeco Modified Eagle Medium (DMEM). BHK-21 cells used to determine JEV plaques were grown in a minimum essential medium (MEM) supplemented with 10% fetal bovine serum (FBS). For analysis, human lung epithelial A549 cells were grown in MEM with 2 mM L-glutamine, 1mM sodium pyruvate and 10 % FBS, whereas human promonocyte HL-CZ cells were incubated with RPMI 1640 medium containing 10 % FBS.

2.2. Detection of apoptosis by flow cytometry

Both uninfected and infected cells with multiplicity of infections (MOIs) of 0.1 and 1 were harvested after 24-, 48-, 72- or 96-hour incubation, respectively. Cells were fixed using 70% ethanol at 4°C overnight, then re-suspended in PBS containing 50 μg/mL PI and 0.1 mg/mL RNase and 0.1% Triton X-100 in darkroom. After 30 min incubation at 37 °C, cells were tested by flow cytometry (Becton-Dickinson, San Jose, CA, USA) equipped with an argon ion laser at 488 nm wavelength, then the apoptotic rates of cells were determined [14, 15].

2.3. Western blotting analysis

Lysates harvested from uninfected and infected cells were dissolved in 2X SDS-PAGE sample buffer without 2-mercaptoethanol, and boiled for 10 min. As

described in a prior report [13], lysate proteins were separated on 12% SDS-PAGE gels and transferred to nitrocellulose paper. Resultant blots were blocked with 5% skim milk, then reacted with properly diluted monoclonal antibodies anti-caspase 3, anti-caspase 8, anti-caspase 9, anti-Grp78 (Cell Signaling Technology), anti-thioredoxin (Sigma), anti-cyclophilin A, anti-ERK1/2, anti-phospho-ERK1/2, anti-p38 MAPK, anti-phospho-p38 MAPK (Cell Signaling Technology) and anti-β-actin, respectively. The immune complexes were detected using horseradish peroxidase-conjugated goat anti-mouse IgG antibodies followed by enhanced chemiluminescence reaction (Amersham Pharmacia Biotech).

2.4. 2-DE and protein spot analysis

Two-dimensional gel electrophoresis and mass spectrum (2D GE/MS) was carried out, as in our earlier report [12]. Cells were infected with JEV at an MOI of 1 and harvested after 72 h incubation. Both uninfected and infected cells were washed twice with ice-cold phosphate-buffered saline, then extracted with lysis buffer containing 8 M urea, 4% CHAPS, 2% pH 3-10 non-linear (NL) IPG buffer (GE Healthcare), and Complete, Mini, EDTA-free protease inhibitor mixture (Roche). After 3 h incubation at 4℃, cell lysates were centrifuged for 15 min at

16000 g. Protein concentration of supernatant was measured with Bio-Rad Protein Assay (Bio-Rad, Hercules, CA, USA). Protein sample of 100 μg was diluted with 350 μl of rehydration buffer (8 M urea, 2% CHAPS, 0.5% IPG buffer pH 3-10 NL, 18 mM dithiothreilol, 0.002% bromophenol blue), then applied to nonlinear Immobiline DryStrips (17 cm, pH 3-10; GE Healthcare). After the run of first-dimensional isoelectric focusing on a Multiphor II system (GE Healthcare), gel strips were incubated for 30 min in equilibration solution I (6 M urea, 2% SDS, 30% glycerol, 1% dithiothreilol, 0.002% bromophenol blue, 50 mM Tris-HCl, pH 8.8) and for another 30 min in equilibration solution II (6 M urea, 2% SDS, 30% glycerol, 2.5% iodoacetamide, 0.002% bromophenol blue, 50 mM Tris-HCl, pH 8.8). Subsequently, IPG gels were moved to the top of 12% polyacrylamide gels (20 cm × 20 cm × 1.0 mm) for secondary dimensional run at 15 mA, 300 V for 14 h. Separated protein spots were fixed in solution (40% ethanol and 10% glacial acetic acid) for 30 min, stained on gel with silver nitrate solution for 20 min, then scanned by GS-800 imaging densitometer with PDQuest software version 7.1.1 (Bio-Rad). Data from three independently stained gels of each sample were exported to Microsoft Excel for creation of the correction graphs, spot intensity graphs, and statistical analysis. Each spot of interest in the silver-stained gel was sliced and put into the microtube, then washed twice with 50% acetonitrile (ACN)

in 100 mM ammonium bicarbonate buffer (pH 8.0) for 10 min at room temperature. Subsequently, the excised-gel pieces were soaked in 100% ACN for 5 min, dried in a lyophilizer for 30 min and rehydrated in 50 mM ammonium bicarbonate buffer (pH 8.0) containing 10g/mL trypsin at 30℃ for 16 h. After digestion, peptides were extracted from supernatant of gel elution solution (50% ACN in 5.0% trifluoroacetic acid), and dried in vacuum centrifuge. Proteins were identified using Ultimate capillary LC system (LC Packings, Amsterdam) coupled to a QSTARXL quadrupole-time of flight (Q-TOF) mass spectrometer (Applied Biosystem/MDS Sciex, Foster City, CA, USA). Peptides were separated by RP C18 capillary column (15 cm×75 μm i.d.) with a flow rate of 200 nL/min, then eluted with a linear ACN gradient from 10-50% ACN in 0.1% formic acid for 60 min. Eluted peptides from the column were sprayed into a mass spectrometer by a PicoTip electrospray tip (FS360-20-10-D-20; New Objective, Cambridge, MA, USA). Data acquisition from Q-TOF was performed via automatic Information Dependent Acquisition (IDA; Applied Biosystem/MDS Sciex). Proteins were identified by nanoLC-MS/MS spectra by searching against NCBI databases for exact matches, using ProID (Applied Biosystem/MDS Sciex) and MASCOT search (http://www.matrixscience.com). *Homo sapiens* taxonomy restriction was used and the mass tolerance of both precursor ion and fragment ions was set to ±

0.3 Da. Carbamidomethyl cysteine was set as a fixed modification, while serine, threonine, tyrosine phosphorylation and other modifications were set as variable modifications. Protein function and subcellular location were annotated using the Swiss-Prot (http://us.expasy.org/sprot/). Proteins were also categorized according to their biological process and pathway, using PANTHER Classification system (http://www.pantherdb.org), as in our previous studies [12].

2.5. Detecting intracellular reactive oxygen species (ROS) by flow cytometry

Uninfected and infected cells at MOI of 1 determined ROS level; 5×10^5 cells were harvested after 48-h transfection and their ROS level noted. They were washed twice with PBS, then incubated with 10 μM 2,7-dichlorodihydrofluorescein diacetate (DCFH-DA, Sigma) at 37°C for 30 min in darkroom for final analysis by flow cytometry (Becton Dickinson FACS Calibur) [14].

3. Results

3.1. JEV-induced caspase 3-mediated apoptosis

To assess the relation between virus replication and apoptosis, we examined JEV replication in human promonocyte HL-CZ cells, human A549 cells and African green monkey kidney Vero cells (Supplementary Fig. S1). These cells were infected

with JEV at MOI of 1, then virus titers of cultured media that were harvested at 12, 24, and 48 hours post-infection (hpi) were determined by plaque assay (Supplementary Fig. S1). *In vitro* growth kinetics revealed cell sensitivity of JEV growth in HL-CZ cells higher than that in A549 cells, lower than that in Vero cells. To investigate the apoptotic response to JEV infection, human promonocyte HL-CZ cells were infected at MOIs of 0.1 and 1 respectively, then apoptosis effects were examined at 0, 24, 48, and 72 hpi by propidium iodide (PI)-stained flow cytometry, showing percentages of apoptosis (sub-G1 group of cell cycles) induced by JEV greatly increased in dose- and time-dependent manners (Fig. 1). Western blotting assays indicated that JEV infection in HL-CZ cells induced activation of caspases 3, 8, and 9 and increment of Grp78 protein (Fig. 2). Replication of JEV in human promonocyte HL-CZ cells increased Grp78 protein induction and activation of caspases 3, 8, and 9, resulting in apoptosis.

3.2. Apoptosis-related protein profiles induced by JEV

For proteome profiling of infected cells, comparative proteomic analysis between uninfected (Fig. 3A) and infected HL-CZ cells (Fig. 3B) was performed by 2D-GE/MS strategy. Protein profiling revealed that 17 up-regulated proteins (Spot ID number 1-17) showed statistically significant 1.5-fold rise in spot intensity, while 17

down-regulated proteins (Spot ID number 18-34) had statistically significant 1.5-fold decrease in JEV-infected cells (Fig. 3). Enlarged images of selected protein spots were used to indicate marked differences between uninfected and infected cells (Fig. 3C). The up- and down-regulated proteins were selected for in-gel tryptic digestion, then underwent peptide mass fingerprinting via NanoLC Trap Q-TOF MS. Representative peptide peaks from Q-TOF MS analysis arose—e.g., heat shock protein 27 (Hsp27, Spot ID 15) (Supplementary Fig. S2A) and thioredoxin (Spot ID 23) (Supplementary Fig. S2B)—resulting in confident protein identification by Mascot searching. Search results indicated that identified up-regulated and down-regulated proteins showed the best match, with a protein score of greater than or equal to 67, considered significant using MASCOT search algorithm ($p < 0.05$) (Supplementary Tables S1 and S2). The amino acid sequence coverage of identified up- and down-regulatory proteins varied from 6% to 81%. Heat shop protein 27 (Spot ID 15) tallied a Mascot score of 207, sequence coverage of 42%, and 6 matched peptides, while thioredoxin (Spot ID 23) showed a Mascot score of 378, sequence coverage of 65%, and 3 matched peptides. Quantitative change of cyclophilin A (Spot ID 10) and thioredoxin (Spot ID 23) were further confirmed by Western blotting with β-actin as internal control (Fig. 4). After normalizing with β-actin, densitometric analysis of immunoreactive-bands of infected cells, cyclophilin A appeared up to a 4.4-fold increase, whereas thioredoxin decreased

by 2.1-fold 48 hours post infection (Fig. 4), in general consistent with proteomic analyses. Comparative analysis of profiling indicated 17 up- and 17 down-regulated proteins in JEV-infected cells.

3.3. Functional classification of up- and down-regulated proteins in infected cells

To assess the possible mechanism of apoptosis induced by JEV, these up- and down-regulated proteins were also categorized according to subcellular location, biological function, biological process and biological pathway using the PANTHER Classification system (Supplementary Fig. S3, Tables S1-S2). Localization was diverse but mainly in the cytoplasm (about 50%). Biological process categorization revealed diversity of processes associated with identified proteins (Supplementary Fig. S3, Tables S1-S2), including antioxidation and free radical removal, carbohydrate metabolism, cell motility, glycolysis, mRNA splicing, pre-mRNA processing, protein biosynthesis, protein complex assembly, protein folding, protein metabolism and modification, pyrimidine metabolism and translation regulation for up-regulated, as well as anion transport, apoptosis, calcium mediated signaling, cation transport, cell proliferation and differentiation, cell structure, constitutive exocytosis, homeostasis, purine metabolism, receptor protein serine/threonine kinase signaling pathway, sulfur metabolism, and sulfur redox metabolism for down-regulated proteins. Up-regulation

was associated with biological pathways of glycolysis, *de novo* purine biosynthesis, pyruvate metabolism and p38 MAPK pathway. Down-regulation was involved in the biological pathways like Wnt signaling, oxidative stress response, hypoxia response, dopamine receptor mediated signaling, glycolysis, *de novo* purine biosynthesis and cytoskeletal regulation. These observations indicated JEV-infected cells triggering global and diverse responses.

3.4. Relationship of oxidative stress and JEV-induced apoptosis

According to protein profiling of the JEV-infected cells, thioredoxin (Spot ID 23) was involved in biological processes of stress response and apoptosis plus a biological pathway of oxidase stress response (Supplementary Table S2) suggested to correlate with JEV-induced apoptosis. Down-regulation of thioredoxin reportedly correlates with heightened levels of reactive oxygen species (ROS) production [15]. We are curious to elucidate whether the intracellular ROS production is related to JEV-induced apoptosis; intracellular ROS production was subsequently analyzed and quantified by flow cytometric methods with DCFH-DA (Fig. 5). At 24 and 48 hours post infection, ROS production in JEV-infected cells proved tenfold that of un-infected cells, demonstrating that JEV led to ROS-mediated apoptosis of HL-CZ

cells and correlate with thioredoxin down-regulation in infected cells. This finding concurs with antioxidation, free radical removal, and sulfur redox metabolism in infected cells (Fig 5, Supplementary Tables S1 and S2), consistent with a previous report that JEV induced a change in mitochondrial potential and the generation of ROS in mouse neuroblastoma cells [7].

3.5. Activation of ASK1 and p38 MAPK in JEV-induced apoptosis

Thioredoxin has been cited as directly inhibiting proapoptotic protein ASK1 activity and level of thioredoxin-ASK1 complex regulated ROS-mediated MAPK pathway activity in cell apoptosis [15]. Here protein levels of ASK1, ERK1/2, phospho-ERK1/2, p38 MAPK and phosphor-p38 MAPK were rated, using Western blotting (Fig. 6). ASK1 expression in infected cells rose with time; Western blotting showed much higher phosporylation levels of ERK1/2 and p38 MAPK protein in JEV-infected cells. ERK/p38 MAPK inhibitor PD98059 treatment reduced apoptotic level of infected cells from 13.2% to 8.9% 2 days post infection (Supplementary Fig. S4), proving ROS-mediated activation of ASK1-ERK/p38 MAPK signaling in JEV-infected cells, correlating with ROS-mediated apoptosis via thioredoxin-ASK1 complex and ERK/p38 MAPK signaling pathways.

4. Discussion

This study demonstrated JEV infection in human promonocytes activating caspases 3, 8, and 9; higher levels of Grp78 protein, stress-induced phosphoprotein 1 and heat shock protein 27; along with increased intracellular ROS generation causing apoptosis. Caspase-dependent apoptosis of human promonocyte HL-CZ cells to JEV infection conformed with JEV-induced apoptosis in human neuroblastoma cells [8], human medulloblastoma cells [16], human hepatocellular liver carcinoma cells [17], and mouse neuroblastoma cells [10]. Greater expression of chaperones Grp78 protein, stress-induced phosphoprotein 1, and heat shock protein 27 in infected promonocytes led to ER stress-mediated apoptosis (Fig. 2, Supplementary Table S1), consistent with JEV-induced ER stress-mediated apoptosis in fibroblast, BHK-21 cells and neuronal cells [10] and GRP78 upregulation in DENV-infected cells [18]. Rise in intracellular ROS level in infected cells correlated with down-regulation of ATP synthase delta chain, thioredoxin, and superoxide dismutase [Cu-Zn], all responsible for activating oxidative stress response pathway in infected cells (Fig 5, a Supplementary Table S2), agreeing with JEV-induced ROS-mediated apoptosis of mouse neuroblastoma and human neuronal cells [7, 19]. Results pointed to involvement of ER stress, ROS, and oxidative stress response in JEV-induced apoptosis.

Activated ASK1, RK1/2 and p38 MAPK in infected cells were involved in

JEV-induced caspase-dependent apoptosis. MAP Kinase (ERK1/2 and p38 MAPK) inhibitor PD98059 treatment starkly inhibited JEV-induced apoptosis (Supplementary Fig. S4). ASK1-MAP kinase (ERK1/2 and p38 MAPK) signal pathway was activated in infected cells, correlating with induction of apoptotic responses by ER stress, ROS and oxidative stress in infected cells, the latter of which activated ASK1-MAP kinase signal pathways [15, 20-22]. ASK1 also proved essential for endoplasmic reticulum stress-mediated apoptosis [22, 23]; ASK1-ERK1/2 signaling pathway was shown to protect cells from ER stress-mediated apoptosis [24]. Involvement of ERK1/2 signal in apoptosis remains unclear. Recently, cytosolic retention of ERK1/2 showed binding with transcription factor substrates, preventing mitogenic responses and inhibiting survival and proliferative signals [25]. Whether JEV-induced apoptosis involves the ASK1-ERK1/2 signaling pathway merits further study.

Unique proteome profiling yielded insight into caspase-dependent apoptosis mechanisms. Biological process categorization revealed antioxidation and free radical removal up-regulated but sulfur redox metabolism down-regulated in infected cells (Supplementary Fig. S3). Proteomics analysis of JEV-infected HL-CZ cells indicated expression changes of apoptosis-related proteins like annexin A1 (Spot ID 2) [26], cyclophilin A (Spot ID 10) [27], heat shock protein 27 (Spot ID 15) [28], voltage-dependent anion channel protein 2 (Spot ID 18) [29],

translationally-controlled tumor protein (Spot ID 21) [30], thioredoxin (Spot ID 23) [31], and Cu/Zn superoxide dismutase (Spot ID 28) [32]. Up-regulation of annexin A1 was reportedly involved in regulation of apoptosis [26]. Greater annexin A1 protein expression also correlated with p38 MAPK activation in butyrate-induced apoptosis of colon adenocarcinoma cells [33]. Cyclophilin A (Spot ID 10) identified as up-regulated protein could interact with apoptosis-inducing factor (AIF), required for nuclear translocation of AIF during apoptosis *in vitro* [27]. Interestingly, up-regulated antioxidant enzyme peroxiredoxin 5 (Spot ID 11) showed reduced intracellular ROS production, leading to prevent apoptosis [34]. Also, translationally-controlled tumor protein (TCTP, Spot ID 21), an anti-apoptotic protein to inhibit Bax dimerization [35], was down-regulated, but down-regulation of cellular antioxidant enzyme superoxide dismutase [Cu-Zn] (Spot ID 28) and the anti-oxidative stress protein DJ-1 (Spot ID 30) resulted in decreased ROS scavenging, implicating generation of ROS and activation of p38-MAPK in induced apoptosis [32, 36]. Most biological processes identified in infected cells were associated with oxidative stress-mediated apoptosis, portending oxidative stress responses might be predominant in JEV-induced apoptosis.

We thus illustrated how JEV replication in human promonocyte cells caused apoptosis through activation of caspases 3, 8 and 9, plus increased Grp78 expression. Comparative proteomic analysis revealed apoptosis-related biological processes and

pathways in JEV-infected cells. JEV infection induced down-regulation of thioredoxin, leading to oxidative stress-mediated apoptosis. Higher intracellular ROS level and activation of ASK1-MAPK (ERK1/2 and p38 MAPK) signaling likewise correlated with JEV-induced apoptosis. This study shows cellular and molecular effects of JEV infection in human promonocytes, valuable insight for development of novel therapeutics against JEV infection.

Acknowledgements

We would like to thank China Medical University and National Science Council, Taiwan for financial support (CMU97-140, CMU97-343, CMU97-CMC-020, and NSC96-2320-B-039-008-MY3).

References

[1] D. S. Burk and T. P. Monath, Flaviviruses In Fields Virology, 4th edn, (2001) pp. 1043-1125. Edited by D. M. Knipe, & P. M. Howley. Philadephia: Lippincott-Raven.

[2] B. D. Lindenbach, C. M. Rice, Flaviridae: the viruses and their replication. In Fields Virology, 4th edn, (2001) pp. 991-1041. Edited by D. M. Knipe, & P. M. Howley. Philadephia: Lippincott-Raven.

[3] T. Solomon, N. M. Dung, R. Kneen, M. Gainsborough, D. W. Vaughn, V. T. Khanh, Japanese encephalitis, J. Neurol. Neurosurg. Psychiatry 68 (2000)

405-415.

[4] T. F. Tsai, Factors in the changing epidemiology of Japanese encephalitis and West Nile fever. In: Saluzzo JF, Dodet B, eds. Factors in the emergence of arbovirus diseases. (1997) pp. 179-189, Paris: Elselvier.

[5] A. Ghoshal, S. Das, S. Ghosh, M.K. Mishra, V. Sharma, P. Koli, E. Sen, A. Basu, Proinflammatory mediators released by activated microglia induces neuronal death in Japanese encephalitis, Glia 55 (2007) 483-496.

[6] C. J. Chen, J. H. Chen, S. Y. Chen, S. L. Liao, S. L. Raung, Upregulation of RANTES gene expression in neuroglia by Japanese encephalitis virus infection, J. Virol. 78 (2004) 12107-12119.

[7] R. J. Lin, C. L. Liao, Y. L. Lin, Replication-incompetent virions of Japanese encephalitis virus trigger neuronal cell death by oxidative stress in a culture system, J. Gen. Virol. 85 (2004), 521–533.

[8] V. Swarup, J. Ghosh, S. Das, A. Basu, Tumor necrosis factor receptor-associated death domain mediated neuronal death contributes to the glial activation and subsequent neuroinflammation in Japanese encephalitis, Neurochem. Int. 52 (2008) 1310-1321.

[9] C. H. Tsao, H. L. Su, Y.L. Lin, H.P. Yu, S.M. Kuo, C.I. Shen, C.W. Chen, C.L. Liao, Japanese encephalitis virus infection activates caspase-8 and -9 in a FADD-independent and mitochondrion-dependent manner, J. Gen. Virol. 89 (2008) 1930-1941.

[10] H.L. Su, C.L. Liao, Y.L. Lin, Japanese encephalitis virus infection initiates endoplasmic reticulum stress and an unfolded protein response, J. Virol. 76 (2002) 4162–4171.

[11] V. Dhingra, Q. Li, A. B. Allison, D. E. Stallknechtm, Z.F. Fu, Proteomic Profiling and Neurodegeneration in West-Nile-Virus-Infected Neurons, J. Biomed.

Biotechnol. 2005 (2005) 271–279.

[12] C. C. Lai, M.J. Jou, S.Y. Huang, S.W. Li, L. Wan, F. J. Tsai, C.W. Lin, Proteomic analysis of up-regulated proteins in human promonocyte cells expressing severe acute respiratory syndrome coronavirus 3C-like protease, Proteomics 7 (2007) 1446-1460.

[13] C. W. Lin, H.D. Huang, S.Y. Shiu, W.J. Chen, M.H. Tsai, S.H. Huang, L. Wan, Y.J. Lin, Functional determinants of NS2B for activation of Japanese encephalitis virus NS3 protease, Virus Res. 127 (2007) 88-94.

[14] S. S. Lin, H. P. Huang, J. S. Yang, J.Y. Wu, T.C. Hsai, C. C. Lin, C.W. Lin, C.L. Kuo, W. Gibson Wood, J.G. Chung, DNA damage and endoplasmic reticulum stress mediated curcumin-induced cell cycle arrest and apoptosis in human lung carcinoma A-549 cells through the activation caspases cascade- and mitochondrial-dependent pathway, Cancer Lett. 272 (2008) 77-90.

[15] C. C. Hsieh, J. Papaconstantinou, Thioredoxin-ASK1 complex levels regulate ROS-mediated p38 MAPK pathway activity in livers of aged and long-lived Snell dwarf mice, FASEB J. 20 (2006) 259-268.

[16] T. C. Yang, S. L. Shiu, P. H. Chuang, Y. J. Lin, L. Wan, Y. C. Lan, C. W. Lin, Japanese encephalitis virus NS2B-NS3 protease induces caspase 3 activation and mitochondria-mediated apoptosis in human medulloblastoma cells, Virus Res. 143 (2009) 77-85.

[17] S. O. Chen, T. J. Chang, G. Stone, C. H. Chen, J. J. Liu, Programmed cell death induced by Japanese encephalitis virus YL vaccine strain or its recombinant envelope protein in varied cultured cells, Intervirology 49 (2006) 346-351.

[18] S. Wati, M. L. Soo, P. Zilm, P. Li, A. W. Paton, C. J. Burrell, M. Beard, J. M. Carr, Dengue virus infection induces upregulation of GRP78, which acts to chaperone viral antigen production. J. Virol. 83 (2009) 12871-80.

[19] M. K. Mishra, D. Ghosh, R. Duseja, A. Basu, Antioxidant potential of Minocycline in Japanese Encephalitis Virus infection in murine neuroblastoma cells: correlation with membrane fluidity and cell death. Neurochem. Int. 54 (2009) 464-470.

[20] H. Nagai, T. Noguchi, K. Takeda, H. Ichijo, Pathophysiological roles of ASK1-MAP kinase signaling pathways. J. Biochem. Mol. Biol. 40 (2007) 1-6.

[21] S. Yamagishi, T. Matsumoto, T. Numakawa, D. Yokomaku, N. Adachi, H. Hatanaka, M. Yamada, K. Shimoke, T. Ikeuchi, ERK1/2 are involved in low potassium-induced apoptotic signaling downstream of ASK1-p38 MAPK pathway in cultured cerebellar granule neurons. Brain Res. 1038 (2005) 223-30.

[22] D. Saggioro, M. P. Rigobello, L. Paloschi, A. Folda, S. A. Moggach, S. Parsons, L. Ronconi, D. Fregona, A. Bindoli, Gold(III)-dithiocarbamato complexes induce cancer cell death triggered by thioredoxin redox system inhibition and activation of ERK pathway. Chem. Biol. 14 (2007) 1128-1139.

[23] Y. Sekine, K. Takeda, H. Ichijo, The ASK1-MAP kinase signaling in ER stress and neurodegenerative diseases. Curr. Mol. Med. 6 (2006) 87-97.

[24] C. Hung, T. Ichimura, J. Stevens, J. Bonventre, Protection of renal epithelial cells against oxidative injury by endoplasmic reticulum stress preconditioning is mediated by ERK1/2 activation. J. Biol. Chem. 278 (2003) 29317–29326.

[25] Y. Mebratu, Y. Tesfaigzi, How ERK1/2 activation controls cell proliferation and cell death: Is subcellular localization the answer? Cell Cycle. 8 (2009) 1168-1175.

[26] M. Scannell, M. B. Flanagan, A. deStefani A, K. J. Wynne, G. Cagney, C. Godson, P. Maderna, Annexin-1 and peptide derivatives are released by apoptotic cells and stimulate phagocytosis of apoptotic neutrophils by macrophages, J Immunol. 178(2007) 4595-4605.

[27] C. Zhu, X. Wang, J. Deinum, Z. Huang, J. Gao, N. Modjtahedi, M. R. Neagu, M.

Nilsson, P. S. Eriksson, H. Hagberg, J. Luban, G. Kroemer, K. Blomgren, Cyclophilin A participates in the nuclear translocation of apoptosis-inducing factor in neurons after cerebral hypoxia-ischemia, J. Exp. Med. 204 (2007) 1741-1748.

[28] D. Singh, K. L. McCann, F. Imani, MAPK and heat shock protein 27 activation are associated with respiratory syncytial virus induction of human bronchial epithelial monolayer disruption, Am. J. Physiol. Lung Cell Mol. Physiol. 293 (2007) L436-L445.

[29] V. Shoshan-Barmatz, A. Israelson, D. Brdiczka, S.S. Sheu, The voltage-dependent anion channel (VDAC): function in intracellular signalling, cell life and cell death, Curr. Pharm. Des. 12 (2006) 2249-2270.

[30] S. H. Chen, P.S. Wu, C.H. Chou, Y. T. Yan, H. Liu, S.Y. Weng, H.F. Yang-Yen, A knockout mouse approach reveals that TCTP functions as an essential factor for cell proliferation and survival in a tissue- or cell type-specific manner, Mol. Biol. Cell. 18 (2007) 2525-2532.

[31] C. Tian, P. Gao, Y. Zheng, W. Yue, X. Wang, H. Jin, Q. Chen, Redox status of thioredoxin-1 (TRX1) determines the sensitivity of human liver carcinoma cells (HepG(2)) to arsenic trioxide-induced cell death, Cell Res. 18 (2008) 458–471

[32] I. Vouldoukis, V. Sivan, M.C. Vozenin, C. Kamaté, A. Calenda, D. Mazier, B. Dugas, Fc-receptor-mediated intracellular delivery of Cu/Zn-superoxide dismutase (SOD1) protects against redox-induced apoptosis through a nitric oxide dependent mechanism, Mol. Med. 6 (2000) 1042-1053.

[33] E. Lecona, J. I. Barrasa, N. Olmo, B. Llorente, J. Turnay, M. A. Lizarbe, Upregulation of annexin A1 expression by butyrate in human colon adenocarcinoma cells: role of p53, NF-Y, and p38 mitogen-activated protein kinase, Mol. Cell Biol. 28 (2008) 4665-4674.

[34] J. Yuan, G. A. Murrell, A. Trickett, M. Landtmeters, B. Knoops, M.X. Wang, Overexpression of antioxidant enzyme peroxiredoxin 5 protects human tendon cells against apoptosis and loss of cellular function during oxidative stress, Biochim. Biophys. Acta. 1693 (2004) 37-45.

[35] L. Susini, S. Besse, D. Duflaut, A. Lespagnol, C. Beekman, G. Fiucci, A.R. Atkinson, D. Busso, P. Poussin, J.C. Marine, J.C. Martinou, J. Cavarelli, D. Moras, R. Amson, A. Telerman, TCTP protects from apoptotic cell death by antagonizing bax function, Cell Death Differ. 15 (2008) 1211-1220.

[36] A. Sekito, S. Koide-Yoshida, T. Niki, T. Taira, S. M. Iguchi-Ariga, H. Ariga, DJ-1 interacts with HIPK1 and affects H2O2-induced cell death. Free Radic. Res. 40 (2006) 155-165.

Figure legends

Fig. 1. Apoptotic induction of JEV in HL-CZ human promonocyte cells. Cells were infected with JEV at MOIs of 0.1 and 1. After 0-, 24-, 48-, and 72-h incubation, cells were harvested, fixed in 70% ethanol at -20°C over night, washed with PBS, then stained with solution containing 50 μg/ml propidium iodide and 50 μg/ml RNase A, stained cells analyzed for apoptosis of JEV-infected cells via propidium iodide flow cytometric assay. Ratio of apoptotic cells was calculated sing flow cytometry.

Fig. 2. Western blotting analysis of caspase 3, caspase 8, caspase 9 and Grp78 in cells infected with JEV. Cells were infected with JEV at MOIs of 0.1 and 1 for 48 h. Each lysate from infected cells was analyzed by 12% SDS-PAGE, then electrophorectically transferred onto nitrocellulose paper. Blot was probed with specific monoclonal antibodies and HRP-conjugated anti-mouse IgG antibodies, immunoreactive bands developed by enhanced chemiluminescence reaction.

Fig. 3. Two-dimensional gel electrophoresis image for total cell extracts from un-infected (A) versus JEV-infected cells (B). 100μg of protein sample was diluted with 350 μl of rehydration buffer, then applied to nonlinear Immobiline DryStrip (17 cm, pH 3-10). After incubation in equilibration solutions, IPG gels were transferred to the top of 12% polyacrylamide gels (20 cm × 20 cm × 1.0 mm). Finally, 2-DE gels were stained with silver nitrate solution. Interesting protein spots showing significant expression differences enlarged (C). Circles indicated protein spots of total cell extracts from un-infected (left) and infected cells (right). Protein size markers were shown at the left of each gel in kDa. Spot ID numbers were consistent to those in Supplementary Tables S1 and S2.

Fig. 4. Western blot analysis of cyclophilin A and thioredoxin in un-infected cells and JEV-infected cells. Cells were infected with JEV at a MOI of 1 for 24h or 48 h, then harvested. The blot was probed with specific monoclonal antibodies and HRP-conjugated anti-mouse IgG antibodies. Immunoreactive bands were developed by enhanced chemiluminescence reaction.

Fig. 5. Flow cytometric analysis of reactive oxygen species (ROS) in JEV-infected cells. Un-infected (A and C) and JEV-infected cells with an MOI of 1 for 24 h (B) or 48 h (D) were harvested, then stained by DCFH-DA dye. The fluorescence intensity of stained cells was determined by flow cytometry and

relative DCF fluorescence of each group, as in part (E). *p< 0.05.

Fig. 6. Western blotting analysis of ASK1, ERK1/2, p38 MAPK, along with phosphorylation of ERK1/2 and p38 MAPK. Cells were infected with JEV at a MOI of 1 for 24h or 48 h, then harvested. The blot was probed with specific monoclonal antibodies and HRP-conjugated anti-mouse IgG antibodies, the immunoreactive bands developed by enhanced chemiluminescence reaction.

Fig. 1

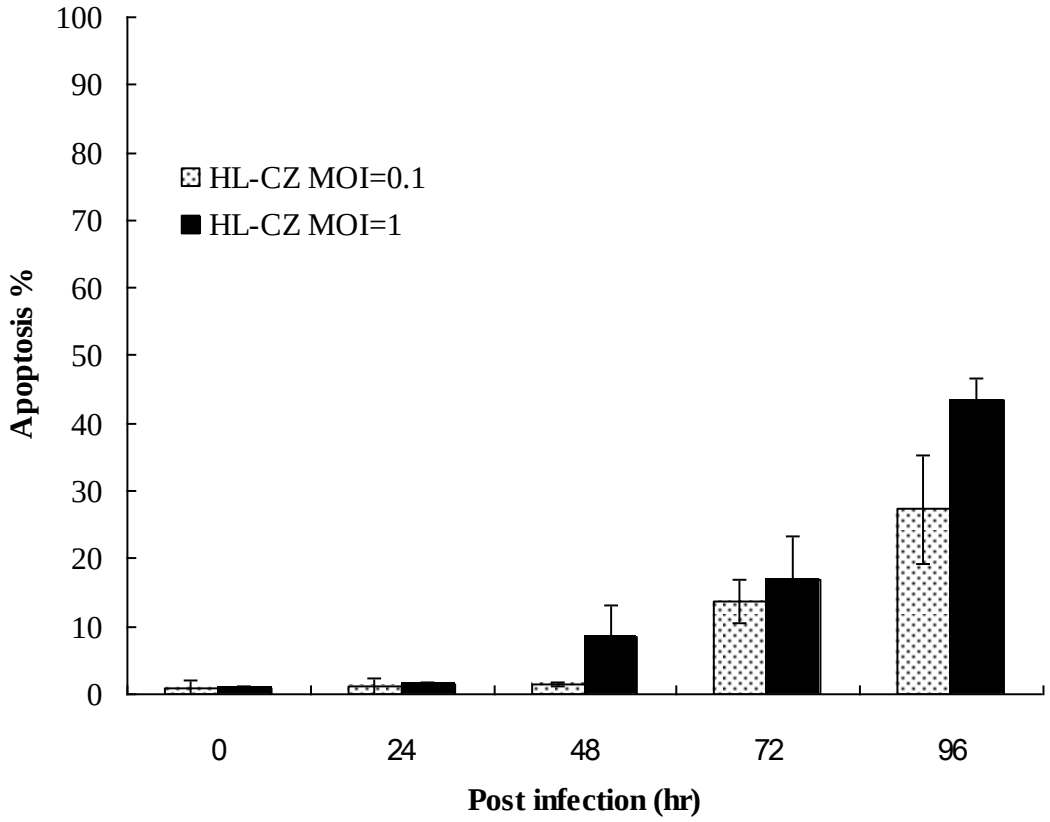
100
90
80
70
60
50
40
30
20
10
0
Apoptosis %
HL-CZ MOI=0.1
HL-CZ MOI=1
0
24
48
72
96
Post infection (hr)

Fig. 2

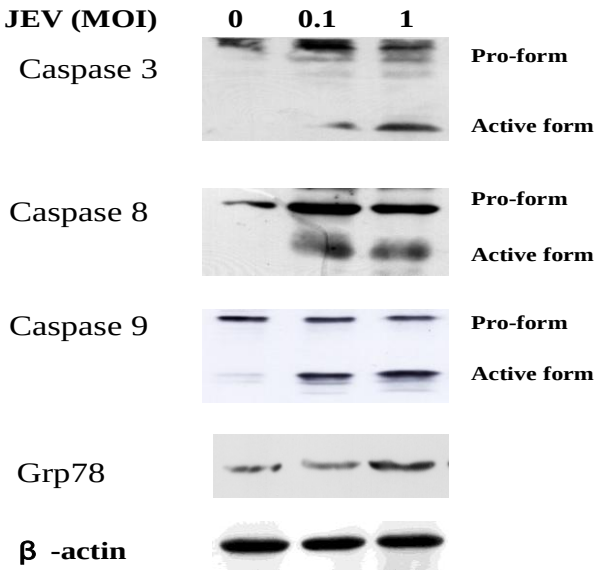
JEV (MOI)
0
0.1
1
Caspase 3
Pro-form
Active form
Caspase 8
Pro-form
Active form
Caspase 9
Pro-form
Active form
Grp78
β -actin

Fig. 3A.

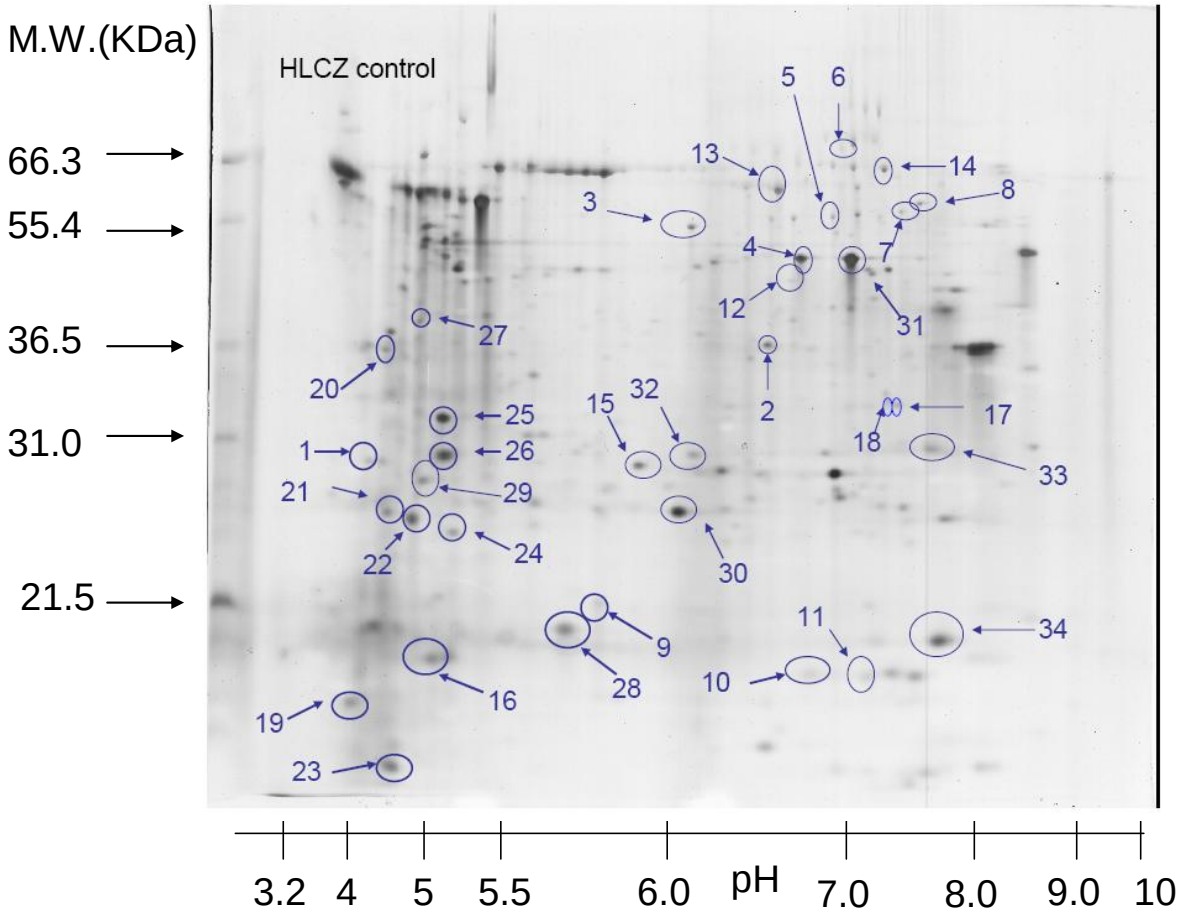
M.W.(KDa)
66.3
55.4
36.5
31.0
21.5
HLCZ control
1
2
3
4
5
6
7
8
9
10
11
12
13
14
15
16
17
18
19
20
21
22
23
24
25
26
27
28
29
30
31
32
33
34
3.2
4
5
5.5
6.0
pH
7.0
8.0
9.0
10

Fig. 3B.

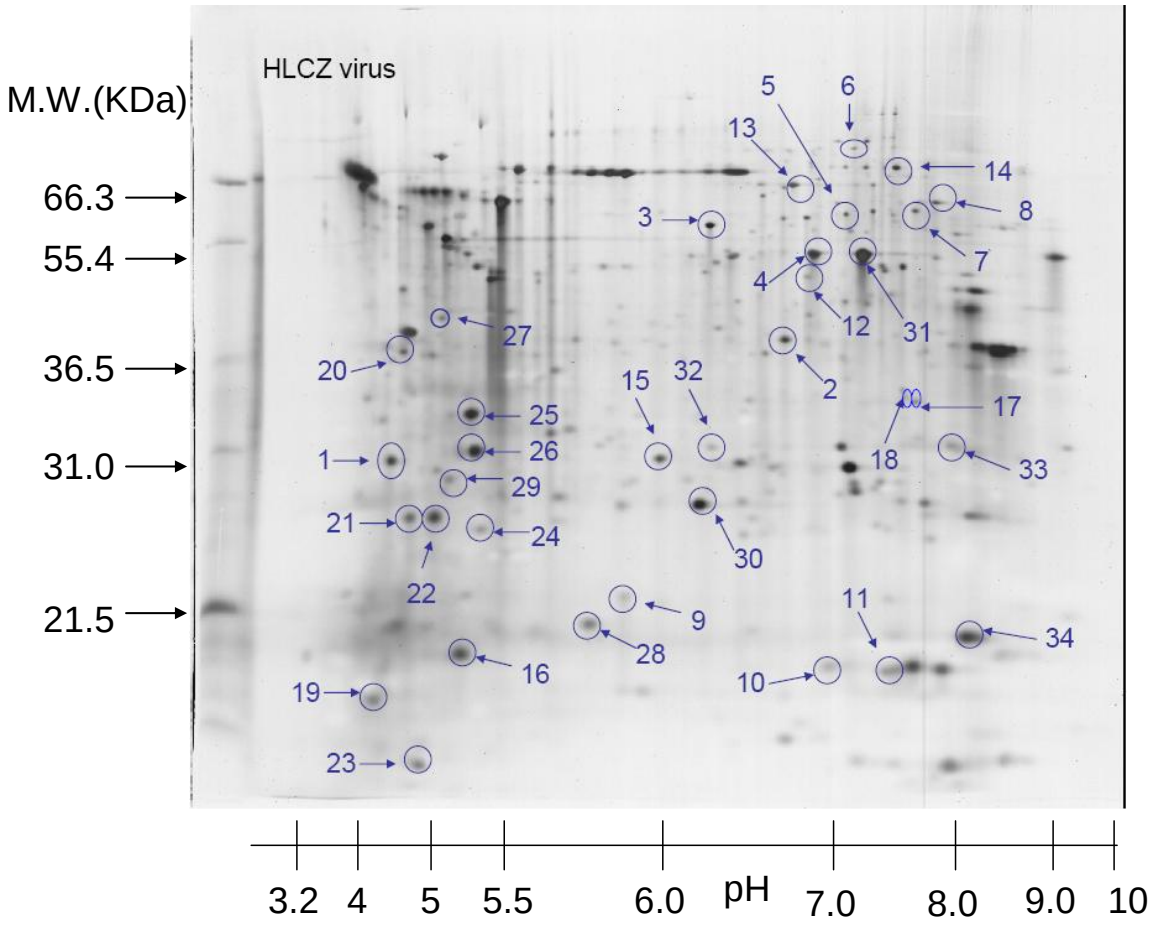

Fig. 3C.

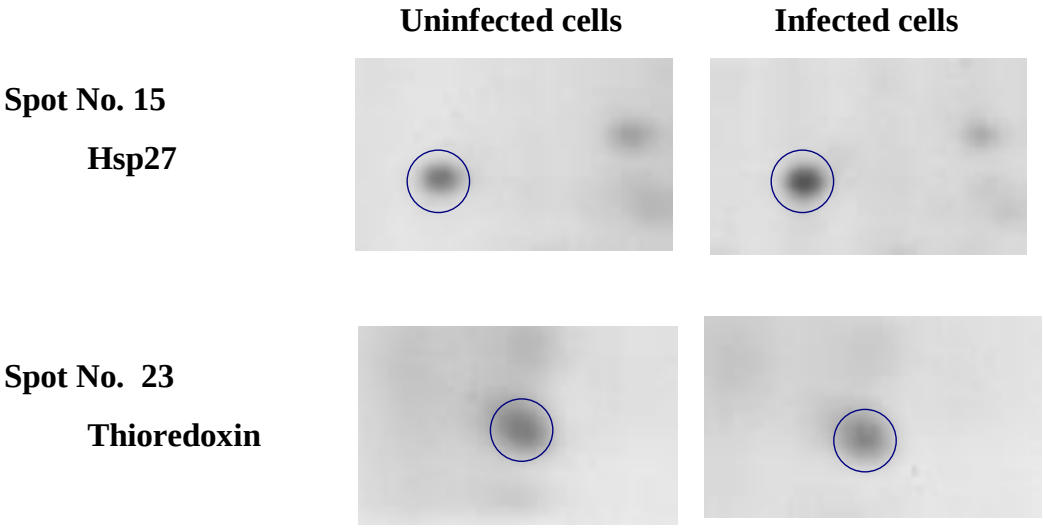
Uninfected cells
Infected cells
Spot No. 15
Hsp27
Spot No. 23
Thioredoxin

Fig. 4

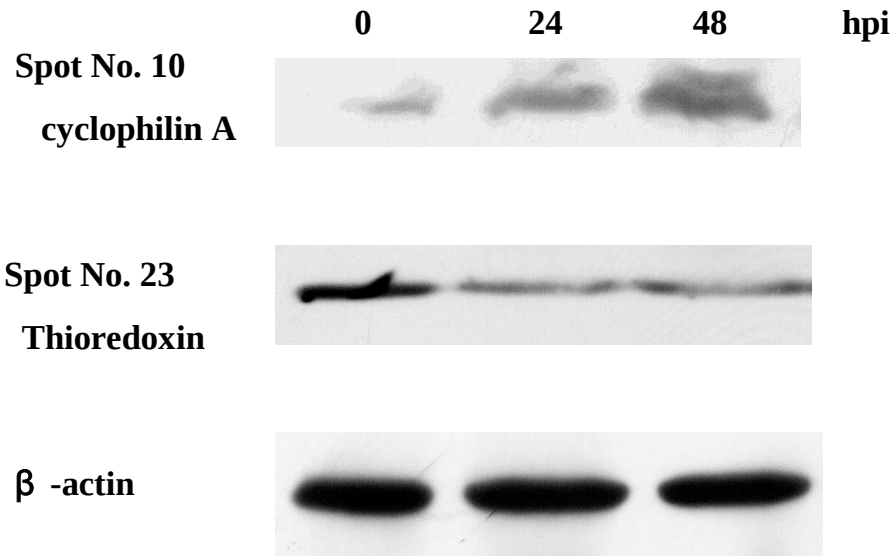
0
24
48
hpi
Spot No. 10
cyclophilin A
Spot No. 23
Thioredoxin
β -actin

Fig. 5 A-D

A.

B.

24 hpi

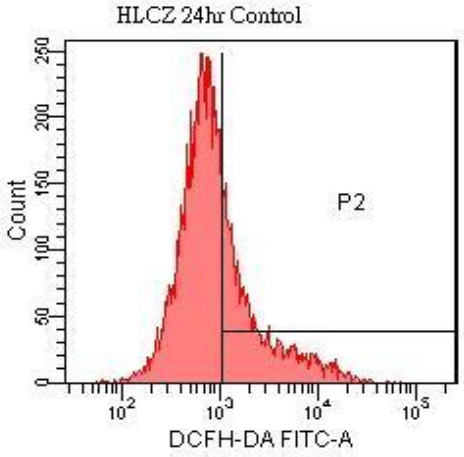

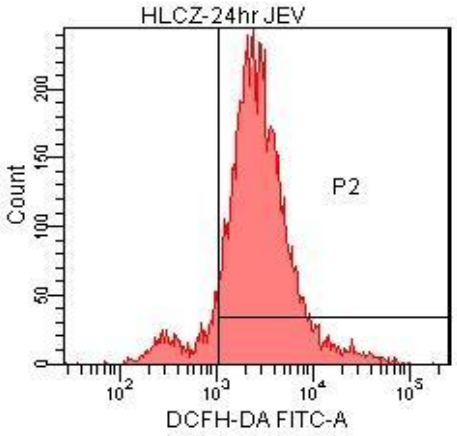

C.

D.

48 hpi

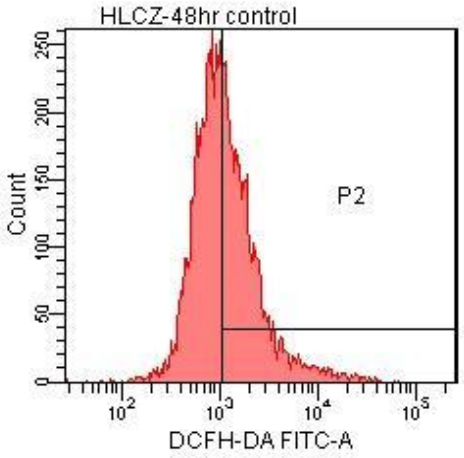

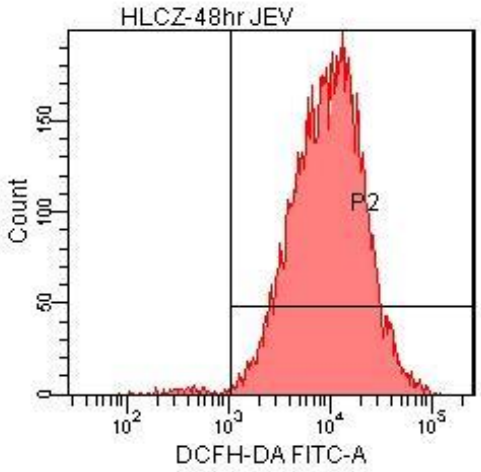

Fig. 5E

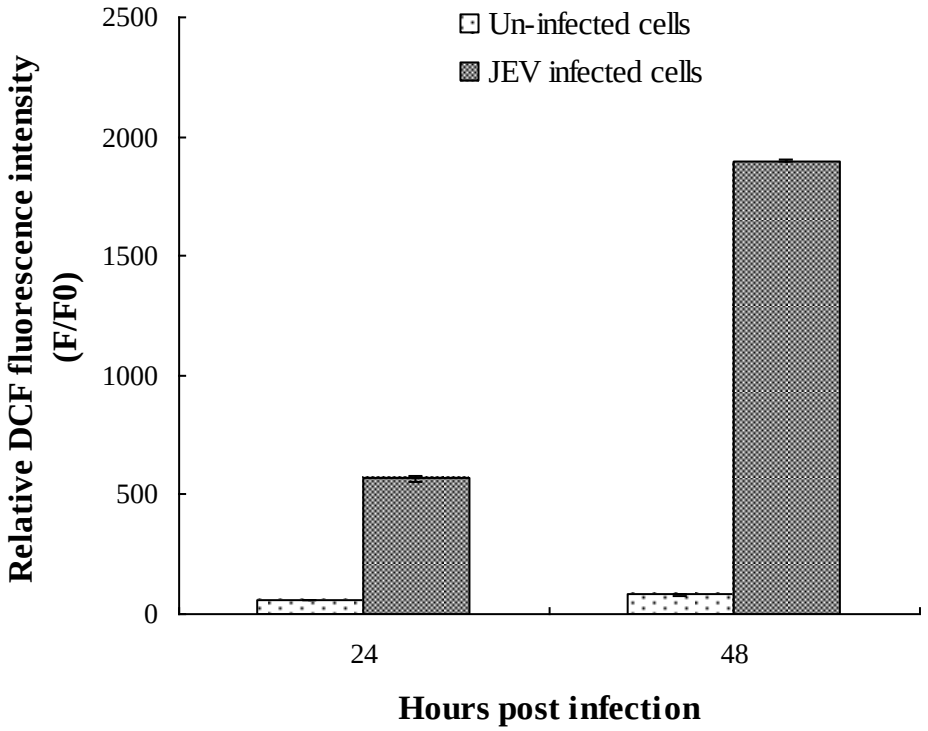
Un-infected cells
JEV infected cells
Relative DCF fluorescence intensity (F/F0)
2500
2000
1500
1000
500
0
24
48
Hours post infection

Fig. 6

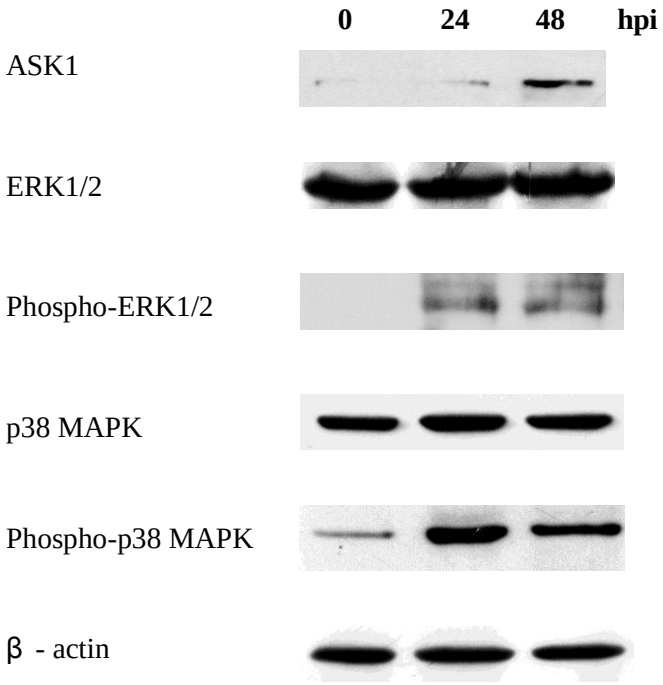
0
24
48
hpi
ASK1
ERK1/2
Phospho-ERK1/2
p38 MAPK
Phospho-p38 MAPK
β - actin

e-component

Click here to download e-component: 20100208-Supplementary data.doc

Dear Reviewers,

Thank you ever so much for this chance to revise our manuscript for publication in *Microbes and Infection*. Our manuscript, "Japanese encephalitis virus down-regulates thioredoxin and induces ROS-mediated ASK1-ERK/p38 MAPK activation in human promonocyte cells," has been previously assigned Number MICINF-D-09-00249. The revised manuscript has clarified writing and description/discussion of data. In addition, it has been corrected according to Reviewer's comments, then carefully edited for grammar, punctuation, spelling, and correct word usage by a native English speaker.

Responses to Reviewer's comments are as follows:

1. The result would fit well with the previously demonstrated JEV-induced endoplasmic reticulum stress (their ref. 10), though the possible intersection of this stress response and oxidative stress is not discussed further in the Discussion. The results are also clearly presented in figures and tables. It is, however, not clear what made the authors look at the ERK1/2 expression. There is too much repetition/reiteration of the results in the Discussion—possible at the expense of a more thorough discussion of the data.

   We have connected the results presented with previously published work in the Discussion section (Pages 15-18) in the revised manuscript, listed as the following:
   "This study demonstrated JEV infection in human promonocytes activating caspases 3, 8, and 9; higher levels of Grp78 protein, stress-induced phosphoprotein 1 and heat shock protein 27; along with increased intracellular ROS generation causing apoptosis. Caspase-dependent apoptosis of human promonocyte HL-CZ cells to JEV infection conformed with JEV-induced apoptosis in human neuroblastoma cells [8], human medulloblastoma cells [16], human hepatocellular liver carcinoma cells [17], and mouse neuroblastoma cells [10]. Greater expression of chaperones Grp78 protein, stress-induced phosphoprotein 1, and heat shock protein 27 in infected promonocytes led to ER stress-mediated apoptosis (Fig. 2, Supplementary Table S1), consistent with JEV-induced ER stress-mediated apoptosis in fibroblast, BHK-21 cells and neuronal cells [10] and GRP78 upregulation in DENV-infected cells [18]. Rise in intracellular ROS level in infected cells correlated with down-regulation of ATP synthase delta chain, thioredoxin, and superoxide dismutase [Cu-Zn], all responsible for activating oxidative stress response pathway in infected cells (Fig 5, a Supplementary Table S2), agreeing with JEV-induced ROS-mediated apoptosis of mouse neuroblastoma and human neuronal cells [7, 19]. Results pointed to involvement of ER stress, ROS, and oxidative stress response in JEV-induced apoptosis.
   Activated ASK1, RK1/2 and p38 MAPK in infected cells were involved in JEV-induced caspase-dependent apoptosis. MAP Kinase (ERK1/2 and p38

MAPK) inhibitor PD98059 treatment starkly inhibited JEV-induced apoptosis (Supplementary Fig. S4). ASK1-MAP kinase (ERK1/2 and p38 MAPK) signal pathway was activated in infected cells, correlating with induction of apoptotic responses by ER stress, ROS and oxidative stress in infected cells, the latter of which activated ASK1-MAP kinase signal pathways [15, 20-22]. ASK1 also proved essential for endoplasmic reticulum stress-mediated apoptosis [22, 23]; ASK1-ERK1/2 signaling pathway was shown to protect cells from ER stress-mediated apoptosis [24]. Involvement of ERK1/2 signal in apoptosis remains unclear. Recently, cytosolic retention of ERK1/2 showed binding with transcription factor substrates, preventing mitogenic responses and inhibiting survival and proliferative signals [25]. Whether JEV-induced apoptosis involves the ASK1-ERK1/2 signaling pathway merits further study.

Unique proteome profiling yielded insight into caspase-dependent apoptosis mechanisms. Biological process categorization revealed antioxidation and free radical removal up-regulated but sulfur redox metabolism down-regulated in infected cells (Supplementary Fig. S3). Proteomics analysis of JEV-infected HL-CZ cells indicated expression changes of apoptosis-related proteins like annexin A1 (Spot ID 2) [26], cyclophilin A (Spot ID 10) [27], heat shock protein 27 (Spot ID 15) [28], voltage-dependent anion channel protein 2 (Spot ID 18) [29], translationally-controlled tumor protein (Spot ID 21) [30], thioredoxin (Spot ID 23) [31], and Cu/Zn superoxide dismutase (Spot ID 28) [32]. Up-regulation of annexin A1 was reportedly involved in regulation of apoptosis [26]. Greater annexin A1 protein expression also correlated with p38 MAPK activation in butyrate-induced apoptosis of colon adenocarcinoma cells [33]. Cyclophilin A (Spot ID 10) identified as up-regulated protein could interact with apoptosis-inducing factor (AIF), required for nuclear translocation of AIF during apoptosis *in vitro* [27]. Interestingly, up-regulated antioxidant enzyme peroxiredoxin 5 (Spot ID 11) showed reduced intracellular ROS production, leading to prevent apoptosis [34]. Also, translationally-controlled tumor protein (TCTP, Spot ID 21), an anti-apoptotic protein to inhibit Bax dimerization [35], was down-regulated, but down-regulation of cellular antioxidant enzyme superoxide dismutase [Cu-Zn] (Spot ID 28) and the anti-oxidative stress protein DJ-1 (Spot ID 30) resulted in decreased ROS scavenging, implicating generation of ROS and activation of p38-MAPK in induced apoptosis [32, 36]. Most biological processes identified in infected cells were associated with oxidative stress-mediated apoptosis, portending oxidative stress responses might be predominant in JEV-induced apoptosis."

2. The manuscript will need considerable English language (grammar & syntax) editing, and it is recommended the authors seek assistance from a native speaker.

   The revised manuscript has been corrected according to Reviewer's comments, then carefully edited for grammar, punctuation, spelling, and correct word usage by an English expert.

3. As many readers of the journal may not be familiar with the methodology, the graphic display used and interpretation of flow cytometric assessment of apoptosis

(Fig 1A), it is recommended that further details are given either in the figure legend or in the text. Otherwise Fig. 1A may be meaningless to many readers of Microbes & Infection.

We deleted Fig. 1A in the revised manuscript. Detailed methodology of apoptosis analysis with PI staining flow cytometric assay was added to the figure legend, listed as the following:
"Fig. 1. Apoptotic induction of JEV in HL-CZ human promonocyte cells. Cells were infected with JEV at MOIs of 0.1 and 1. After 0-, 24-, 48-, and 72-h incubation, cells were harvested, fixed in 70% ethanol at -20°C over night, washed with PBS, then stained with solution containing 50 μg/ml propidium iodide and 50 μg/ml RNase A, stained cells analyzed for apoptosis of JEV-infected cells via propidium iodide flow cytometric assay. Ratio of apoptotic cells was calculated sing flow cytometry."

Thanks very much again!

Sincerely,

Cheng-Wen Lin, PhD
Professor
Department of Medical Laboratory Science and Biotechnology
China Medical University